Thermochimica Acta, 129 (1988) 197–215
Elsevier Science Publishers B.V., Amsterdam – Printed in The Netherlands

PHASE CHANGES ON HEATING AMMONIUM MAGNESIUM PHOSPHATE HYDRATES

B.E.I. ABDELRAZIG and J.H. SHARP

Department of Ceramics, Glasses and Polymers, University of Sheffield, Sheffield (Gt. Britain)

(Received 16 September 1987)

ABSTRACT

DTA and TG curves of $NH_4MgPO_4 \cdot 6H_2O$, $NH_4MgPO_4 \cdot H_2O$ and $(NH_4)_2Mg(HPO_4)_2 \cdot 4H_2O$ are complex because of several overlapping reactions and different reaction paths, dependent on the combination of phases present and the experimental variables, especially the atmosphere. By heating samples to various temperatures, quenching to room temperature and examining the reaction products by X-ray diffraction, the phases formed after various heat treatments have been identified. The most important reaction sequence on heating in the presence of excess MgO is

$$\begin{tikzcd}
NH_4MgPO_4 \cdot 6H_2O \arrow[dr] & & & & \\
 & NH_4MgPO_4 \cdot H_2O \arrow[r] & \text{amorphous phase} \arrow[r] & Mg_2P_2O_7 \arrow[r, "+MgO"] & Mg_3(PO_4)_2 \\
(NH_4)_2Mg(HPO_4)_2 \cdot 4H_2O \arrow[ur, "+MgO"] & & & &
\end{tikzcd}$$

INTRODUCTION

There is considerable current interest in ammonium magnesium phosphate hydrates. They have been found in the human bladder and kidney stones [1], as minerals associated with guano [2–4], in cans of crabmeat [5] and salmon [6], in dental cements [7–9], and in recently developed, rapid-setting cements recommended for repair work [10–14]. The chemistry of these cement systems has been the subject of several recent papers and it is established that ammonium magnesium phosphate hexahydrate (or struvite) $MgNH_4PO_4 \cdot 6H_2O$ is the major hydration product, which can be accompanied by at least two other ammonium magnesium phosphate hydrates, $MgNH_4PO_4 \cdot H_2O$ and $Mg(NH_4)_2(HPO_4)_2 \cdot 4H_2O$, and a sodium ammonium phosphate hydrate, $NaNH_4HPO_4 \cdot 4H_2O$. Struvite or "hexahydrate" is also an important compound in the qualitative identification and gravimetric determination of magnesium [15].

0040-6031/88/$03.50

These four phosphate hydrates give complicated X-ray diffraction patterns, and when mixtures of two or more of them are present identification can be difficult [11–14]. Thermal methods are useful complementary techniques for the identification of phases present in such mixtures, but once again the curves obtained from mixtures of hydrates are complex. It is important, therefore, to be able to identify the cause of the various peaks that appear on heating these hydrates. Furthermore, these magnesia–phosphate cements (MPC) may prove to be good refractory cements and it is essential to understand the phase changes that occur on heating and to know the temperature range in which gases may be evolved.

There is little published information concerning the thermal decomposition of these hydrates, although $MgNH_4PO_4 \cdot 6H_2O$ was the subject of several investigations earlier this century [16–19]. Whitaker [4] has reported that the subaerial decomposition of struvite leads to the formation of newberyite, $MgHPO_4 \cdot 3H_2O$, whereas Paulik and Paulik [20] reported that $MgNH_4PO_4 \cdot H_2O$ may or may not be formed as a stable reaction intermediate according to the experimental conditions. They also discussed the further changes that occurred on heating samples up to 400 °C.

EXPERIMENTAL

All the samples investigated, with the exception of sample H1, were prepared during a study [21] of the hydration of magnesia–phosphate cement and mortar. The various phases identified, from X-ray diffraction (XRD) traces of the samples, are summarized in Table 1.

The samples designated H are those which contain hexahydrate (or struvite) as the predominant hydration product, whereas those designated T

TABLE 1

XRD analysis of the samples studied

Sample	SiO_2	MgO	ADP	Hexahydrate	Tetrahydrate	Monohydrate	Na-phase
H1	nd	nd	nd	+ +	nd	nd	nd
H2	+ +	+ +	tr	+	nd	nd	tr
H3	+ +	+ +	nd	+ +	tr	nd	nd
T1	nd	+ +	+ +	+	+ +	nd	tr
M1	nd	+ +	tr	nd	nd	+ +	nd
M2	nd	+ +	nd	nd	tr	+ +	nd
M3	nd	+ +	+	nd	+ +	+ +	nd

Key: + + indicates present in substantial amounts; + indicates present in minor amounts; tr indicates present in trace amounts; and nd indicates not detected. ADP = $NH_4H_2PO_4$; hexahydrate = $MgNH_4PO_4 \cdot 6H_2O$; tetrahydrate = $Mg(NH_4)_2(HPO_4)_2 \cdot 4H_2O$; monohydrate = $MgNH_4PO_4 \cdot H_2O$; Na-phase = $NaNH_4HPO_4 \cdot 4H_2O$.

or M contain mostly tetrahydrate (or schertelite) or monohydrate (or dittmarite), respectively. Sample H1 is a pure sample of hexahydrate synthesized according to the procedure described by Vogel [15] using a freshly prepared diammonium hydrogen phosphate $(NH_4)_2HPO_4$ solution added to a solution of magnesium sulphate. Hexahydrate was precipitated by slowly adding pure concentrated ammonia.

Samples H2 and H3 were hydration products of magnesia–phosphate cement (MPC) mortar hydrated for 1 week using a w : s ratio of 1 : 16, and for 1 h using a w : s ratio of 1 : 8, respectively *. Both these samples contain substantial amounts of quartz and unreacted MgO (Table 1). Sample T1 is the hydration product of MPC cement (comprising MgO, ammonium dihydrogen phosphate (ADP) and sodium tripolyphosphate (STPP)) hydrated for 1 week using a w : s ratio of 1 : 8.

Samples M1–M3 are from MPC cement, without STPP, hydrated at a w : s ratio of 1 : 8 for periods of 72 h, 15 min and 1 h, respectively. Samples T1, M1, M2 and M3 all contain a substantial amount of MgO, but because they are free from SiO_2 contain much more of the hydration products than do samples H2 and H3.

The hydration of all these samples was carried out at 22 °C. The dry powder was added to distilled water, which had been decarbonated by boiling and then allowed to cool, except for sample M3 when the water was added to the powder.

The starting materials used (MgO, ADP and STPP) were supplied by FEB (Great Britain) Ltd. XRD analyses indicated the presence of small amounts of impurities in the magnesia including Mg_2SiO_4, $CaMgSiO_4$ and $MgAl_2O_4$. The ADP was shown to be pure, except for the presence of silica in trace amounts. It consisted of spherical particles, 0.5–1 μm in diameter and larger agglomerates of the order of 2–5 μm. The STPP was pure but present in two forms.

The XRD traces were obtained using a Philips PW-1730 diffractometer using monochromatic Cu K_α radiation and a scanning rate of 2° 2θ $\min^{-1}$. DTA curves were obtained using 100-mg samples heated in a Stanton-Redcroft 67-3 or 67-4 apparatus with fired α-alumina as the reference material. The samples were heated at 10 °C $\min^{-1}$ in air or flowing N_2. To comprehend the various peaks observed by DTA and to understand the phase changes with temperature, the samples were heated to a particular temperature, quenched to room temperature and then examined by XRD. TG curves were obtained using 20-mg samples heated at 10 °C $\min^{-1}$ in flowing nitrogen on a Stanton-Redcroft 762 thermobalance.

---

* A mortar comprises cement and sand (or other inert filler) in the approximate ratio of 1 : 3 cement : sand. The w : s ratio is the ratio of water to total solid matter.

RESULTS

Ammonium dihydrogen phosphate $NH_4H_2PO_4$ (ADP)

ADP is frequently present in hydration products of MPC, especially after short periods of hydration. It is necessary, therefore, to know the thermal behaviour of ADP when heated alone. TG analysis indicates that ADP starts to lose mass at about 170 ° C, giving a DTG peak at 215 ° C. The DTA curve shows one sharp endotherm with a peak temperature at 210 ° C, attributed to melting as well as decomposition. The observed loss in mass on heating a sample of ADP under isothermal conditions at 215 ° C compared quite well with that expected from the equation

$$NH_4H_2PO_4 \rightarrow H_3PO_4 + NH_3 \qquad (1)$$

On cooling, this sample was glassy (indicating melting) and amorphous to X-rays. The glass was soluble in water giving a solution with a pH of about 3, in accordance with the formation of H_3PO_4.

MgO + ADP

In magnesia–phosphate cement systems for dental and rapid repair applications magnesia is always present in large excess in the hydrated paste. Sometimes unreacted ADP is also present, so that interaction between these materials may be responsible for some of the peaks obtained when the hydrated samples are examined by thermal analysis techniques.

The DTA curve for a 4 : 3, by weight, anhydrous mixture of MgO : ADP is shown in Fig. 1 curve A, whereas that for a 4 : 2.6 : 0.4, by weight, anhydrous MgO : ADP : STPP mixture is shown in Fig. 1 curve B. The two curves are very similar showing sharp endothermic peaks at 185 and 180 ° C, respectively, which are attributed to melting, followed by broadening at ~ 200 ° C due to the partial decomposition of ADP according to eqn. (1).

The phases observed by XRD after heating samples to various temperatures and quenching to room temperature are summarized in Table 2. The amorphous phase was indicated by a hump in the XRD pattern between 17 and 34° 2θ. It is due to the formation of a glassy phase which may contain H_3PO_4 and melted $NH_4H_2PO_4$. The broad endotherms ~ 300 ° C in Fig. 1 curves A and B are attributed to the formation of $MgNH_4(PO_3)_3$, perhaps by the reaction

$$MgO + NH_4H_2PO_4 + 2H_3PO_4 \rightarrow MgNH_4(PO_3)_3 + 4H_2O \qquad (2)$$

The formation of $Mg(PO_3)_2$, observed by XRD after heating to 450 ° C and quenching to room temperature, may be explained by either eqn. (3) or eqn. (4)

$$MgO + 2H_3PO_4 \rightarrow Mg(PO_3)_2 + 3H_2O \qquad (3)$$

$$MgO + 2MgNH_4(PO_3)_3 \rightarrow 3Mg(PO_3)_2 + 2NH_3 + H_2O \qquad (4)$$

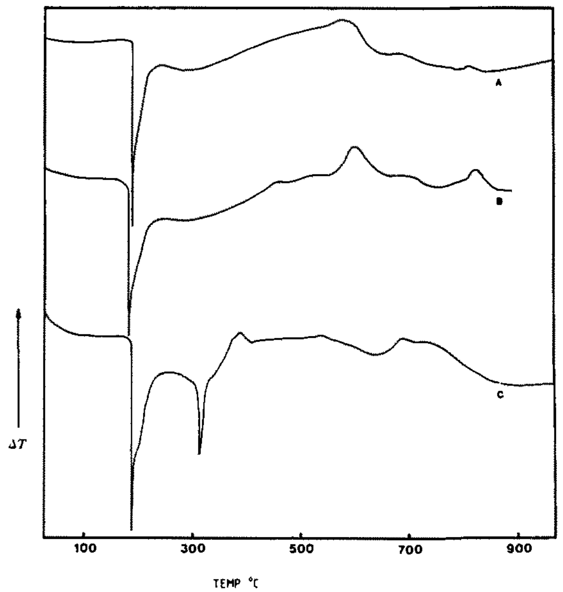

Fig. 1. DTA curves for: (A) $MgO-NH_4H_2PO_4$ anhydrous mixture; (B) $MgO-NH_4H_2PO_4-Na_5P_3O_{10}$ anhydrous mixture; and (C) $MgO-NH_4H_2PO_4$ anhydrous mixture (hand mixed).

Since the amount of $MgNH_4(PO_3)_3$ was observed to increase at 450 °C, reaction (3) seems to be more likely than reaction (4).

The formation of $Mg_2P_2O_7$ (through reactions 5 and 6 below) is responsible for the exotherms at 575 °C (Fig. 1 curve A) and 596 °C (Fig. 1 curve B), whereas the exotherms at 811°C (Fig. 1 curve A) and 820 °C (Fig. 1 curve B) are attributed to the formation of $Mg_3(PO_4)_2$ (eqn. (7))

$$2MgNH_4(PO_3)_3 + 4MgO \rightarrow 3Mg_2P_2O_7 + 2NH_3 + H_2O \tag{5}$$

$$Mg(PO_3)_2 + MgO \rightarrow Mg_2P_2O_7 \tag{6}$$

$$MgO + Mg_2P_2O_7 \rightarrow Mg_3(PO_4)_2 \tag{7}$$

TABLE 2

Phases observed by XRD after heating a 4:3 MgO:ADP anhydrous mixture to various temperatures

Temperature (°C)	Phases observed
140	MgO and ADP
225	MgO and amorphous phase (H_3PO_4 and/or $NH_4H_2PO_4$ glass)
330	MgO, amorphous phase and $MgNH_4(PO_3)_3$
450	MgO, amorphous phase, $MgNH_4(PO_3)_3$ and $Mg(PO_3)_2$
700	$Mg_2P_2O_7$, $Mg(PO_3)_2$
885	$Mg_2P_2O_7$, $Mg(PO_3)_2$, $Mg_3(PO_4)_2$

An endothermic spike superimposed on the broad endotherm ~ 300 °C was observed (Fig. 1 curve C) when a 4 : 3 mixture of MgO : ADP was mixed by hand (not mechanically) for 5 min as usual, prior to heating. This spike is conspicuously absent in the curves shown in Fig. 1 curves A and B. Its cause is not understood, but it is so sharp that it would seem to be associated with the melting of some phase. The small exotherm around 320 °C is attributed to the crystallization of $MgNH_4(PO_3)_3$.

Hexahydrate $MgNH_4PO_4 \cdot 6H_2O$

Pure sample of hexahydrate

The DTA curve for a 10-mg sample of the pure hexahydrate (sample H1) is shown in Fig. 2 curve A. The sample was placed on top of fired α-alumina to make up the weight, and heated to 1000 °C in static air. The sharp well-developed endothermic peak at 103 °C is due to the decomposition of the hexahydrate into the monohydrate, while the broad endotherm at 235 °C is attributed to the decomposition of the monohydrate. The very small exothermic peak around 600 °C is attributed to the formation of $Mg_2P_2O_7$.

The TG and DTG curves for the pure hexahydrate sample, heated in static air up to 1000 °C, are shown in Fig. 3 curves A. A total weight loss of 53.2% was observed in the temperature range 65–750 °C, 90% of which took place between 65 and 250 °C. The DTG curve, however, showed a well-developed peak at 95 °C and diffuse broad peak around 628 °C. The observed weight loss is slightly below the calculated overall weight loss of 54.7% due

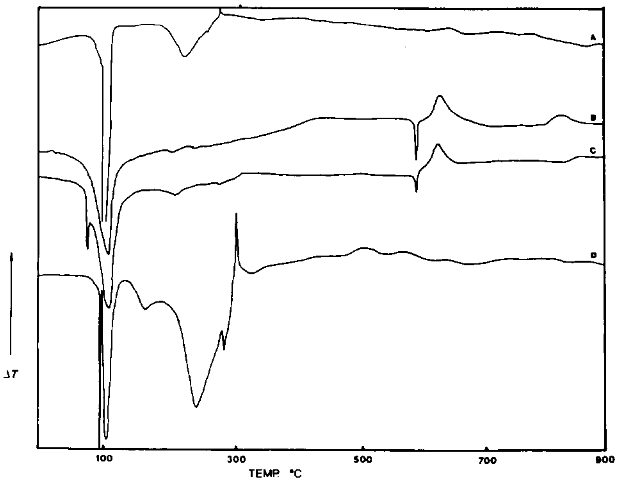

Fig. 2. DTA curves for: (A) pure $NH_4MgPO_4 \cdot 6H_2O$ (sample H1); (B) MPC mortar hydrated for 1 week with a w : s ratio of 1 : 16 (sample H2); (C) MPC mortar hydrated for 1 h with a w : s ratio of 1 : 8 (sample H3); and (D) $MgO–NH_4H_2PO_4–NH_4MgPO_4 \cdot 6H_2O$ anhydrous mixture.

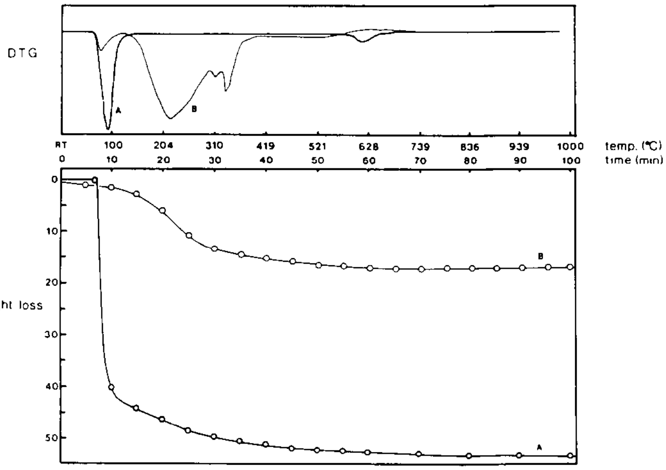

Fig. 3. TG curves for: (A) pure $NH_4MgPO_4 \cdot 6H_2O$ (sample H1); and (B) $MgO-NH_4H_2PO_4$ mixture hydrated for 15 min with a w:s ratio of 1:8 (sample M2).

to loss of the water of crystallization ($6H_2O$), ammonia and the constitutional water.

The possible decomposition reactions in this complex process are reported by Paulik and Paulik [20] to be

$$MgNH_4PO_4 \cdot 6H_2O \rightarrow MgNH_4PO_4 \cdot H_2O + 5H_2O(\text{water of crystallization}) \tag{8}$$

with expected weight loss of 36.7%

$$MgNH_4PO_4 \cdot H_2O \rightarrow MgNH_4PO_4 + H_2O(\text{water of crystallization}) \tag{9}$$

with expected cumulative weight loss of 44.1%

$$MgNH_4PO_4 \rightarrow MgHPO_4 + NH_3 \tag{10}$$

with expected cumulative weight loss of 51.0%

$$MgHPO_4 \rightarrow \tfrac{1}{2}Mg_2P_2O_7 + \tfrac{1}{2}H_2O(\text{constitutional water}) \tag{11}$$

with expected final cumulative weight loss of 54.7%

In an attempt to examine the pure hexahydrate sample for this proposed mechanism the semi-isothermal (quasi-static) method was used under an atmosphere of flowing nitrogen and in static air. The procedure followed was to heat each sample (~ 10 mg) in the thermobalance at 10 °C min^{-1} up to 100 °C and then to hold isothermally at this temperature until the rate of weight change was observed to reach a minimum, as samples do not readily achieve constant weight even after 10 h. Then the temperature was raised once again at the same rate to 235 °C and kept constant at this temperature until no significant weight loss was observed. Finally it was raised at 10 °C min^{-1} to 1000 °C.

TABLE 3

TG data for sample H1 and XRD data for sample H2

Temperature (°C)	Run 1 [a]	Run 2 [b]	Run 3 [c]	Reaction products (by XRD) [d]	Calculated cumulative loss in mass for various reactions	
					Reaction (see text)	Mass loss (%)
100	40.0	39.4	45.0	M	(8)	36.7
235	47.5	46.1	47.5	M+X	(9)	44.1
300	49.5	50.1	50.8	X	(10)	51.0
750	53.2	53.7	55.0	P	(11)	54.7
1000				O+P	(7)	54.7

[a] static air, 10 °C min^{-1}.

[b] static air, quasi-static heating.

[c] flowing nitrogen, quasi-static heating.

[d] $M = MgNH_4PO_4 \cdot H_2O$; X = amorphous phase; $P = Mg_2P_2O_7$; and $O = Mg_3(PO_4)_2$.

The weight losses obtained when the samples were heated in static air at 10 °C min^{-1} to 1000 °C (Run 1), and those in static air (Run 2) and flowing nitrogen (Run 3) using the semi-isothermal method are shown in Table 3.

The total weight loss in nitrogen was observed to be 55.0%, a value close to the expected weight loss of 54.7%. Slightly lower total weight losses were determined in static air, when the buoyancy conditions differ, but are still in reasonably good agreement with the calculated weight loss.

The weight losses recorded at 100 °C in all the runs are above the calculated weight loss expected due to loss of $5H_2O$. In nitrogen atmosphere (Run 3), however, it is even slightly above the calculated weight loss expected due to loss of $6H_2O$. At 235 °C the weight losses obtained in the three runs are very close to each other and above the weight loss calculated due to $6H_2O$, but are all less than the weight loss expected due to ($6H_2O$ + NH_3), which is not readily reached even at 300 °C.

It was also observed that weight losses obtained in the flowing gas atmosphere were always higher than those under static air conditions. The effect of the vapour pressure in the gas atmosphere immediately in contact with the sample, together with the likely effect that some of the ammonia may be evolved simultaneously with the water of crystallization, may explain the complexity of this process and hence the discrepancies observed.

The DTA curve of sample H2 is shown in Fig. 2 curve B where it is compared with the DTA curve of the pure hexahydrate sample. This sample was heated to various temperatures in the DTA apparatus and then quenched to room temperature, when it was examined by XRD.

The phases observed at temperatures up to 1000 °C are shown in Fig. 4(a). The sodium tetrahydrate phase ($NaNH_4HPO_4 \cdot 4H_2O$) was not detected at 100 °C and is therefore responsible for the

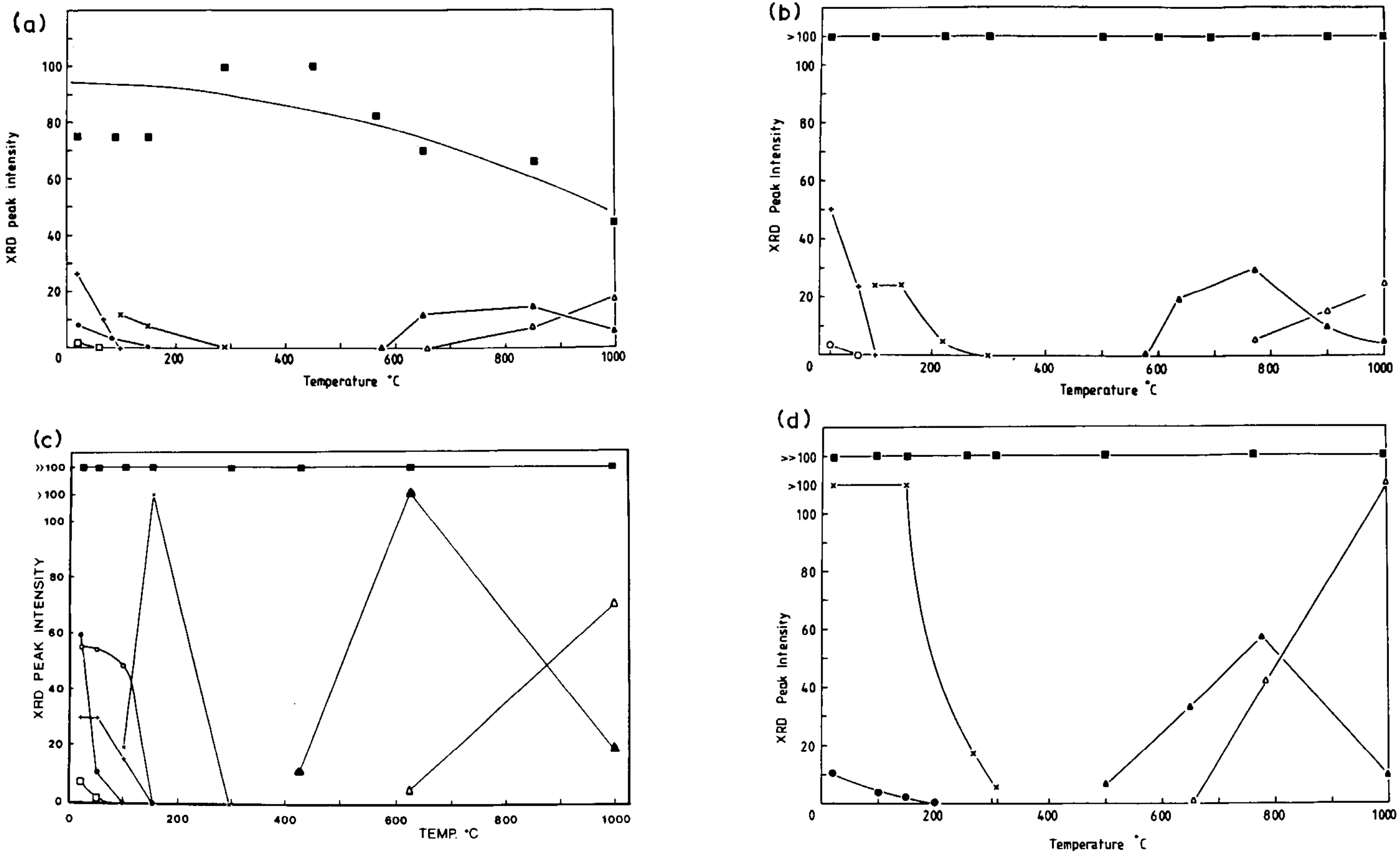

Fig. 4. XRD peak intensities of the phases observed after heating up to the temperatures shown and quenching to room temperature: (a) sample H2; (b) sample H3; (c) sample T1; (d) sample M1; and (e) (shown on the next page) sample M3. Key: ■ MgO; ● $NH_4H_2PO_4$; + $NH_4MgPO_4 \cdot 6H_2O$; ○ $(NH_4)_2Mg(HPO_4) \cdot 4H_2O$; × $NH_4MgPO_4 \cdot H_2O$; ▲ $Mg_2P_2O_7$; △ $Mg_3(PO_4)_2$; □ $NaNH_4(HPO_4) \cdot 4H_2O$.

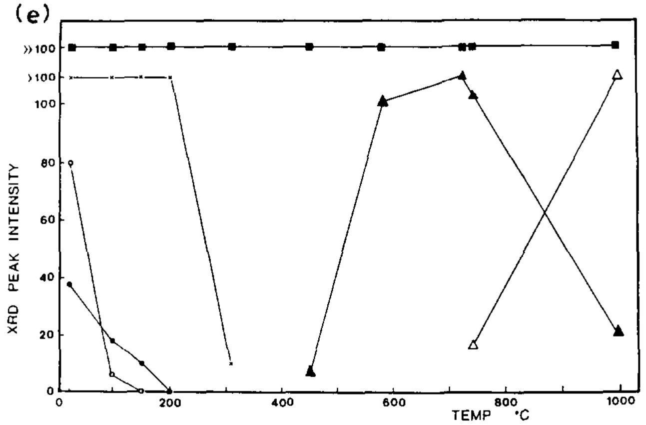

51 °C in Fig. 2 curve B. Unreacted ADP decreased gradually, to disappear by 140 °C. The monohydrate, which was formed during the decomposition of the hexahydrate, decomposes between 200 and 300 °C, giving a small endothermic peak at 232 °C in Fig. 2 curve B, which is more prominent in Fig. 2 curve A. On further heating between 300 and 550 °C an amorphous phase was formed, indicated by an "amorphous hump" in the range 18–32° 2θ in the XRD pattern. This amorphous phase is $MgNH_4PO_4$ and/or $MgHPO_4$ from the decomposition of $MgNH_4PO_4 \cdot H_2O$ according to eqns. (9) and (10) which may overlap significantly, resulting in

$$MgNH_4PO_4 \cdot H_2O \rightarrow MgHPO_4 + NH_3 + H_2O \qquad (12)$$

$Mg_2P_2O_7$ was first observed around 575 °C (eqn. (11)) and reached a maximum at 850 °C, the temperature at which $Mg_3(PO_4)_2$ was first detected. Above 850 °C $Mg_3(PO_4)_2$ continued to increase as $Mg_2P_2O_7$ decreased, up to 1000 °C, in accordance with eqn. (7).

After heating samples to temperatures between 650 and 1000 °C and quenching, additional XRD peaks were observed attributable to mixtures of anhydrous sodium pyrophosphate ($Na_4P_2O_7$) and sodium magnesium phosphates.

The DTA curve of sample H3 is shown in Fig. 2 curve C and the phase changes observed after heating samples to various temperatures and quenching are shown in Fig. 4(b). The behaviour is strikingly similar to that of sample H2, especially above 200 °C where they are almost identical.

The tetrahydrate phase was not detected after heating to 80 °C and may, therefore, be responsible for the sharp endotherm at 87 °C in Fig. 2 curve C. Alternatively, an exotherm peaking ~ 95 °C may be superimposed on a large endotherm due to the decomposition of both the hexahydrate and tetrahydrate phases. This exotherm is believed to be due to the reaction of the tetrahydrate phase with unreacted MgO according to the equation

$$(NH_4)_2Mg(HPO_4)_2 \cdot 4H_2O + MgO \rightarrow 2MgNH_4PO_4 \cdot H_2O + 3H_2O \qquad (13)$$

Although the exotherm is not especially striking in Fig. 2 curve C because the tetrahydrate phase is present only in trace amounts, it was frequently much more clearly observed in other systems to be discussed.

The monohydrate, formed through reaction (13) and from the decomposition of the hexahydrate phase at 100 ° C, decomposed between 200 and 300 ° C. More $Mg_2P_2O_7$ was detected to form than from sample H2, since more hexahydrate was shown to be present because of the higher w : s ratio used in sample H3.

Mixture of hexahydrate–MgO–ADP

It has been shown elsewhere [21] that a typical hydrated magnesia–phosphate cement comprises approximately 45% MgO, 30% hexahydrate and 25% ADP. Such a mixture has been made up using the pure sample of hexahydrate (H1) and examined by DTA (Fig. 2 curve D). What appears at first sight to be a double endotherm at ~ 100 ° C cannot be, since no tetrahydrate (nor indeed any hydrate other than hexahydrate) is present. Rather a sharp exotherm at 100 ° C is superimposed on the very large endotherm peaking at 105 ° C due to the decomposition of hexahydrate. The broad endotherm at 170 ° C is associated with the presence of ADP, probably due to reactions (1) and (2). The major difference from Fig. 2 curves B and C is, however, the large endotherm at 254 ° C, due to the decomposition of monohydrate, which was shown by XRD to be present in large amounts after heating to 140 ° C and quenching to room temperature. It is apparent that the area under the monohydrate peak is greater than that of the peak corresponding to the hexahydrate, indicating that some monohydrate must also be formed, by another route, in addition to that from the decomposition of hexahydrate. It seems, therefore, that the reaction

$$MgO + NH_4H_2PO_4 \rightarrow MgNH_4PO_4 \cdot H_2O \qquad (14)$$

takes place and is the cause of the sharp exotherm observed at 100 ° C.

The endothermic spike observed at 300 ° C is clearly similar to that observed in Fig. 1 curve C, when reaction (2) was also postulated. The sharp exotherm at 325 ° C is presumably due to the crystallization of some phase, perhaps $MgNH_4(PO_3)_3$. The broad exotherms at 552 and 613 ° C are both believed to be due to the formation of $Mg_2P_2O_7$ by two different routes (to be discussed further), while the broad, shallow exotherm at 800 ° C is due to the formation of $Mg_3(PO_4)_2$, which was more prominent in Fig. 2 curve B and other systems.

Tetrahydrate $Mg(NH_4)_2(HPO_4)_2 \cdot 4H_2O$

Sample containing a substantial amount of tetrahydrate from the hydration of MPC

Whereas the hydration of MPC mortar yields hydration products containing mostly hexahydrate, the hydration of MPC cement can lead to products containing mostly tetrahydrate, such as sample T1, which contains unreacted MgO and ADP, some hexahydrate and traces of $NaNH_4PO_4 \cdot 4H_2O$ as well as tetrahydrate. The DTA curve of sample T1 is shown in Fig. 5 curve A and the phases observed after heating the sample to various temperatures and quenching are shown in Fig. 4(c).

No $NaNH_4HPO_4 \cdot 4H_2O$ was detected after heating to 80 °C, and it is therefore responsible for the peak at 51 °C in Fig. 5 curve A. Unreacted ADP was observed to decrease gradually and was not detected at 150 °C or above, which suggests that it may have reacted. The sharp exotherm at 100 °C in Fig. 5 curve A, superimposed on the large endotherm due to the dehydration of both tetrahydrate and hexahydrate, is indicative of the formation of more monohydrate through reactions (13) and (14). The presence of monohydrate in substantial quantities (even though absent in the starting material) is indicated by the large endotherm at 240 °C and was confirmed by XRD of the samples heated between 100 and 200 °C. The tetrahydrate and hexahydrate phases decomposed simultaneously and were not detected by XRD at 150 °C, the temperature at which the monohydrate phase reached a maximum. On further heating an amorphous phase was detected between 300 and 400 °C, indicated by a broad hump in the range 18–34° 2θ in the XRD pattern. $Mg_2P_2O_7$ was first observed by XRD at around 450 °C and reached a maximum around 630 °C, leading to two exotherms at 550 and 617 °C in the DTA curve. At 660 °C XRD indicated the presence of a small amount of $Mg_3(PO_4)_2$, which was observed to increase, while $Mg_2P_2O_7$ decreased, on further heating up to 1000 °C. Additional XRD peaks were observed in the range 665–1000 °C, which are attributed to a mixture of sodium pyrophosphate and sodium magnesium phosphates.

Monohydrate $MgNH_4PO_4 \cdot H_2O$

In the absence of STPP, samples of mostly monohydrate were readily obtained in the $MgO–ADP–H_2O$ cement system. Three such samples were examined, in detail, two by DTA and XRD and one by TG. XRD of sample M1 shows that it contains monohydrate, unreacted MgO and traces of ADP; sample M2 is very similar except that it also contains tetrahydrate; sample M3 contains monohydrate, unreacted MgO and ADP, and some tetrahydrate. The thermal behaviour of samples M1 and M2 is reported as representative of samples consisting almost entirely of monohydrate diluted by

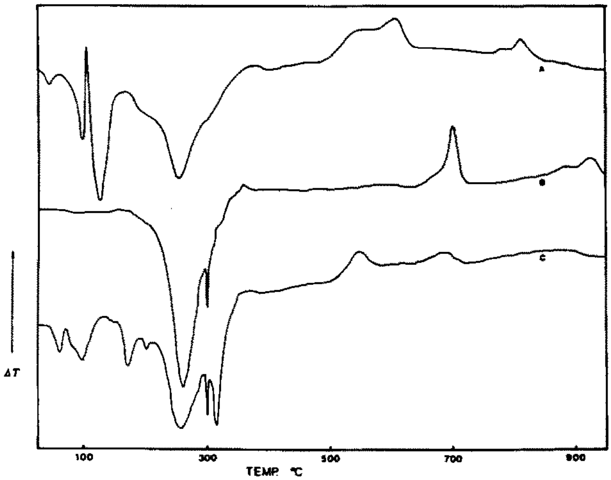

Fig. 5. DTA curves for: (A) MPC cement hydrated for 1 week with a w:s ratio of 1:8 (sample T1); (B) MgO-$NH_4H_2PO_4$ mixture hydrated for 72 h with a w:s ratio of 1:8 (sample M1); and (C) MgO-$NH_4H_2PO_4$ mixture hydrated for 1 h with a w:s ratio of 1:8 (sample M3).

MgO, whereas that of M3 is a sample containing appreciable amounts of monohydrate, contaminated with tetrahydrate and unreacted ADP as well as MgO. The latter is more typical of the complicated patterns associated with hydration products of MPC.

Sample of mostly monohydrate from the hydration of MPC

The DTA curve of sample M1 is shown in Fig. 5 curve B and the phases formed after heating to various temperatures and quenching are shown in Fig. 4(d). ADP was observed to decrease on heating and was not detected at 200 ° C or above. The monohydrate phase decomposed between 200 and 300 ° C, giving a very strong endotherm at 248 ° C as shown in Fig. 5 curve B. The endothermic spike at ~ 300 ° C, also seen in Fig. 1 curve C and Fig. 2 curve D, is evident. Once again reaction products amorphous to XRD were obtained between 320 and 450 ° C. A strong exotherm due to the formation of $Mg_2P_2O_7$ is clearly seen at ~ 700 ° C in Fig. 5 curve B. This phase was first observed by XRD after heating to 500 ° C and continued to increase up to 800 ° C, the temperature at which $Mg_3(PO_4)_2$ was first detected. Above 800 ° C $Mg_2P_2O_7$ was observed to decrease, while $Mg_3(PO_4)_2$ increased in amount up to 1000 ° C. In contrast to samples H2 and T1, no other phases were detected to form above 450 ° C, because of the lack of STPP in the initial mixture which supplied Na ions in the former cases.

The TG and DTG curves of sample M2 are shown in Fig. 3 curves B. The small DTG peak at ~ 90 ° C is attributed to the presence of a small amount of tetrahydrate, whereas the major DTG peak at ~ 220 ° C is due to the decomposition of monohydrate.

The principal reaction taking place during the hydration is

$$MgO + NH_4H_2PO_4 \xrightarrow{H_2O} MgNH_4PO_4 \cdot H_2O \quad (15)$$

i.e. 1 mole of MgO reacts with 1 mole of ADP to form 1 mole of monohydrate. Although no water is needed for the formation of the monohydrate it is necessary for the initiation of the reaction (i.e. by means of a through-solution mechanism).

Since we have used 1.86 moles (75 g) of MgO and 0.49 moles (56.25 g) of ADP, the amount of monohydrate formed = 0.49 × 155.34 = 76.12 g, and the amount of unreacted MgO = 1.37 × 40.31 = 55.23 g. Hence according to equation (15) the final product should consist of 57.95% monohydrate and 42.05% MgO, since the free water was removed when the sample was ground in an excess of AnalaR acetone.

Possible stages in the decomposition of monohydrate are

$$MgNH_4PO_4 \cdot H_2O \rightarrow MgNH_4PO_4 + H_2O \quad (9)$$

with expected weight loss of 6.7% in the above sample (11.60% of the pure monohydrate)

$$MgNH_4PO_4 \rightarrow MgHPO_4 + NH_3 \quad (10)$$

with expected total weight loss of 13.09% in the sample of mostly monohydrate (22.6% of pure monohydrate)

$$MgHPO_4 \rightarrow \tfrac{1}{2}Mg_2P_2O_7 + \tfrac{1}{2}H_2O \quad (11)$$

with final weight loss of 16.4% (28.4% of pure monohydrate).

The calculated total loss in mass of 16.4% can be compared with the observed loss in the TG curve in Fig. 3 curve B of 17.2%, which is higher because of the presence of the small amount of the tetrahydrate phase. It is clear that reactions (9) and (10) overlap significantly. Hence, the temperature at which $MgHPO_4$ is fully formed corresponds to a loss of mass of $17.2 - (16.4 - 13.09) = 13.89\%$, i.e. around 325 °C. This is close to the temperature of the endothermic spike observed in some of the DTA curves (including Fig. 5 curve B) and to the two small but sharp DTG peaks (Fig. 3 curve B). The spike seems likely to be associated with melting (and XRD of samples heated above this temperature always indicated the presence of a glassy phase), while the DTG peaks signify a more rapid evolution of NH_3 and/or H_2O from the melt.

Sample containing a substantial amount of monohydrate from the hydration of MPC

The DTA curve of sample M3 is shown in Fig. 5 curve C and the XRD data obtained after quenching samples heated to various temperatures are summarised in Fig. 4(e). Although the decomposition of monohydrate is clearly evident in the DTA curve (endothermic peak at 258 °C), the presenc of significant amounts of tetrahydrate and unreacted ADP have led to a very complicated DTA trace. These "impurity" phases were observed by XRD to decrease in amount with increasing temperature. Tetrahydrate was not detected at 150 ° C, whereas ADP disappeared after heating to 200 ° C. The low temperature peaks in the DTA curve are all associated with the tetrahydrate phase; it starts to decompose (endothermic peaks at 78 and 104 ° C), but also reacts with MgO to form monohydrate (exotherm at 90 ° C due to reaction (13)). The endotherms at 175 and 200 ° C are attributed to the presence of ADP. The former may be due to the formation of some $MgNH_4(PO_3)_3$ through reaction (2), whereas the latter is due to melting and partial decomposition of ADP. XRD indicated that monohydrate decreased in amount above 200 ° C and was not detected at 330 ° C, confirming that its decomposition is responsible for the large endotherm at 258 ° C. It should be noted that there are two endothermic spikes at 295 and 310 ° C in Fig. 5 curve C. Their causes are not fully understood, but both may be associated with melting, perhaps of $MgNH_4PO_4$ and/or $MgHPO_4$ from the decomposition of monohydrate (cf. Fig. 5 curve B) and $MgNH_4(PO_3)_3$ (cf. Fig. 1 curve C).

On further heating to 1000 ° C the sample behaved in a similar way to sample M1 (compare Fig. 4(e) with Fig. 4(d)). It is interesting, however, to compare the exothermic peaks in Fig. 5 curves B and C. The crystallization of $Mg_2P_2O_7$ is believed to be responsible for both of the exothermic peaks at 550 and 685 ° C in curve C of Fig. 5, whereas only one, relatively strong, exotherm was observed in curve B of Fig. 5 at 700 ° C. This behaviour indicates the formation of $Mg_2P_2O_7$, through two reaction paths in curve C of Fig. 5, from the anhydrous phosphates (perhaps via reactions (4), (5) and (6)) as well as from the decomposition of monohydrate (reaction (11)). Sample M1, however, contained only traces of ADP and no tetrahydrate, so that curve B of Fig. 5 shows only one exotherm associated with the formation of $Mg_2P_2O_7$ from the decomposition of the large amount of monohydrate present. At higher temperatures small exotherms are associated with the formation of $Mg_3(PO_4)_2$ according to eqn. (7).

DISCUSSION

It should be realized that the XRD intensities of the hydrate phases are more intense in Figs. 4(c), (d) and (e) than in Figs. 4(a) and (b), because the former are samples of cement whereas the latter are mortars, i.e. cements effectively diluted with a large amount of silica sand. Another consequence is that the exothermic peaks from the cement samples are larger than those from the mortar samples, simply because of the greater amount of phosphates present.

Although relatively straightforward DTA curves similar to Fig. 2 curves A and B and Fig. 5 curve B are sometimes observed when hydrated MPC samples are examined, Fig. 2 curves C and D, and Fig. 5 curves A and C are more typical of the complex DTA curves frequently obtained. Without an in-depth study of the cause of these various peaks, it would not be possible to use DTA (or indeed DSC or DTG) to characterize the reaction products from these systems. Yet, because the XRD patterns of many of these reaction products are also very complex with many overlapping peaks and the formation of amorphous as well as crystalline phases, the use of complementary techniques such as thermal methods of analysis is vitally important.

The complexity is only in part caused by the number of different phases present in a hydrated sample. A typical sample [13] contains silica (if a mortar), unreacted MgO and ADP, hexahydrate and tetrahydrate. Further complexity arises in the thermal analysis curves for two reasons. First, these phases are liable to interact with one another with formation of other phases that give rise to DTA peaks. Secondly, the reaction sequence followed is strongly dependent upon the experimental conditions. Some examples are given below to illustrate these points.

The principal reaction products in hydrated MPC are hexahydrate and tetrahydrate, which on heating usually follow the reaction sequence in Fig. 6, which is similar to that proposed by Neiman and Sarma [9]. The DTA

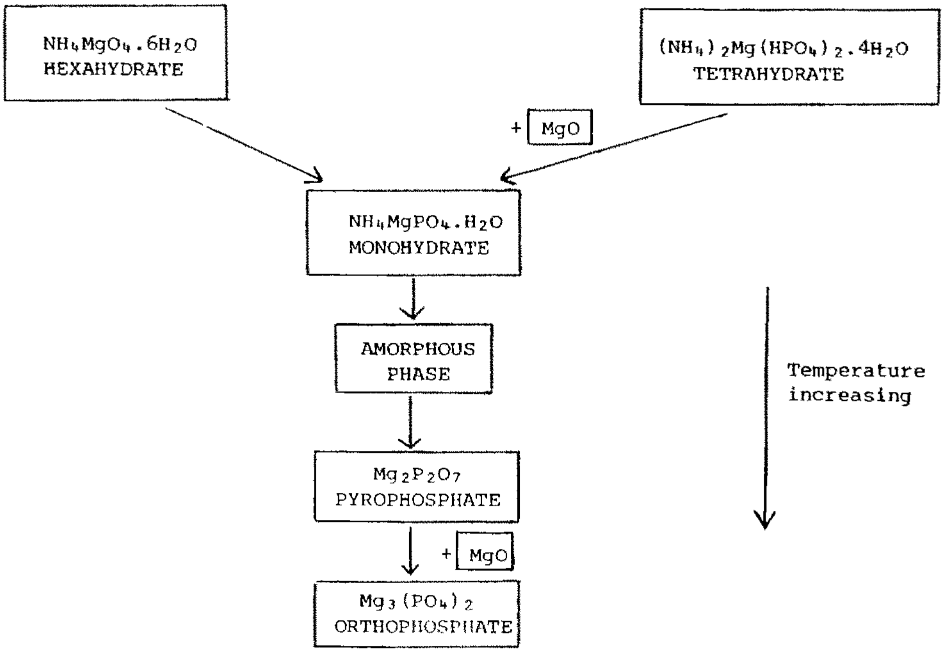

Fig. 6. Reaction sequence on heating ammonium magnesium phosphate hydrates.

curves shown in Fig. 2 curves A and B (hexahydrate) and Fig. 5 curve A (mostly tetrahydrate) can be interpreted in this manner. The DTG curve shown in Fig. 3 curve A, however, indicates that the same sample of hexahydrate as used in obtaining Fig. 2 curve A can, under different experimental conditions, decompose directly to an anhydrous phase without the intermediate formation of the monohydrate phase. A similar observation has been made by Paulik and Paulik [20] using different designs of sample holder. Whether monohydrate is formed is dependent on the back pressure of water vapour that is allowed to build up in the reaction chamber. Thus it was observed in the present work (Table 3) that the loss in mass from hexahydrate is dependent on whether a flowing or static atmosphere is used.

Another uncertainty concerns the nature of the amorphous phase formed from the decomposition of the monohydrate phase. The reaction could occur in sequential steps

$$MgNH_4PO_4 \cdot H_2O \rightarrow MgNH_4PO_4 \rightarrow MgHPO_4 \rightarrow \tfrac{1}{2}Mg_2P_2O_7 \tag{16}$$

or even

$$MgNH_4PO_4 \cdot H_2O \rightarrow MgHPO_4 \cdot H_2O \rightarrow MgHPO_4 \rightarrow \tfrac{1}{2}MgP_2O_7 \tag{17}$$

or one or more of the intermediates may be omitted. Paulik and Paulik [20] suggested that under the experimental conditions of their experiments the reactions are simultaneous, i.e. they can be summarized by the equation

$$2MgNH_4PO_4 \cdot H_2O \rightarrow Mg_2P_2O_7 + 3H_2O + 2NH_3 \tag{18}$$

Under the conditions of our experiments we also believe that the loss of the last molecule of "water of crystallization" and ammonia overlaps. Indeed a preliminary study [22] using evolved gas analysis by means of mass spectrometry has confirmed that water vapour and ammonia are evolved simultaneously between 200 and 300 °C. We believe, however, that the half molecule of "constitutional water" is usually retained until higher temperatures and is lost only gradually on further heating, hence the small DTG peak at 625 °C in Fig. 3 curve A. The loss in mass observed by TG (Fig. 3 and Table 3) suggests that $MgHPO_4$ is the only phase present above 325 °C, which is slightly higher than the temperature at which an endothermic spike is sometimes observed by DTA (e.g. Fig. 5 curve B). This spike is almost certainly associated with a fusion process leading to the formation of the amorphous phase. It seems, therefore, that the composition of the glass is in the $MgHPO_4$–$MgNH_4PO_4$ system with a relatively low NH_3 content, which is readily lost on further heat treatment.

Although the nature and cause of the endothermic peaks in Figs. 2 and 5 have been emphasized, the smaller exotherms observed in all these DTA curves should not be overlooked. The reaction scheme summarized in Fig. 6 indicates the formation of $Mg_2P_2O_7$ and $Mg_3(PO_4)_2$, which were both observed as crystalline phases by XRD. Exotherms associated with the formation of these phases are clearly evident in Fig. 2 curve B and Fig. 5 curve B. It is also apparent, however, that the temperature of the first exotherm can vary by 150 °C or so (compare Fig. 5 curves B and C) and that sometimes double exotherms are evident (e.g. Fig. 5 curve A). Similar exotherms are also present in DTA curves of the anhydrous MgO–ADP reaction series (e.g. Fig. 1 curve B). It seems, therefore, that there are two routes to the formation of $Mg_2P_2O_7$, one via the hydrate phases (Fig. 6) and one via the anhydrous phases (reactions (1), (3) and (6)). The latter route was clearly established when a 4 : 3 (by weight) mixture of MgO : ADP was heated, but it is uncertain to what extent this reaction scheme is followed in hydrated samples. The observation of double exotherms in Fig. 5 curve A and of several "bumps" that may be exothermic peaks in many other DTA curves (e.g. Fig. 2 curve D) strongly suggests that this alternative route to the formation of $Mg_2P_2O_7$ and ultimately to $Mg_3(PO_4)_2$ is also followed.

There is, however, no evidence under the experimental conditions used in this investigation for the formation of newberyite, $MgHPO_4 \cdot 3H_2O$, by the reaction reported by Whitaker [4]

$$MgNH_4PO_4 \cdot 6H_2O \rightarrow MgHPO_4 \cdot 3H_2O + NH_3 + 3H_2O \qquad (19)$$

One of the most interesting features of the present work was the complex behaviour observed at around 100 °C in many DTA curves (e.g. Fig. 2 curve C and Fig. 5 curve A). Although this might at first sight seem to be due to a double endotherm, close inspection of many curves in addition to those shown here indicates that a sharp exotherm occurs superimposed upon a broad endotherm. The intensity of the exotherm varies in accordance with the amount of the tetrahydrate phase observed by XRD [13,21]. Furthermore, wherever the exotherm was observed it was followed at 250 °C by a much larger endotherm due to the presence of more of the monohydrate phase (confirmed by XRD). It is proposed, therefore, that the reaction occurring is

$$MgO + Mg(NH_4)_2(HPO_4)_2 \cdot 4H_2O \rightarrow 2MgNH_4PO_4 \cdot H_2O + 3H_2O \qquad (13)$$

This reaction may occur in two stages

$$Mg(NH_4)_2(HPO_4)_2 \cdot 4H_2O \rightarrow MgNH_4PO_4 \cdot H_2O + NH_4H_2PO_4 + 3H_2O \qquad (20)$$

followed by

$$MgO + NH_4H_2PO_4 \rightarrow MgNH_4PO_4 \cdot H_2O \qquad (14)$$

Reaction (14) is proposed as the explanation for the exotherm observed in Fig. 2 curve D, which is from a system that does not contain tetrahydrate.

With the knowledge gleaned from this study it has been possible to use DTA as a major supporting technique to XRD in a thorough investigation [21] of the hydration products of magnesia–phosphate cements. It is hoped that it will also prove beneficial to scientists studying ammonium magnesium phosphate hydrates in natural products such as urinary calculi, dental cements and minerals.

ACKNOWLEDGEMENTS

We are grateful to FEB (Great Britain) Ltd. for the supply of samples and financial support, to the Government of the Sudan and the British Council for financial support, and to Dr. B. El Jazairi and Mr. H.D. Winbow for helpful discussions.

REFERENCES

1 K. Lonsdale and D.J. Sutor, Science, 154 (1966) 1353.
2 R.W.E. MacIvor, Chem. News, 60 (1887) 215.
3 A.W. Frazier, J.R. Lehr and J.P. Smith, Am. Mineral., 48 (1963) 635.
4 A. Whitaker, Mineral. Mag., 36 (1968) 820.
5 J.A. Bland and S.J. Basinski, Nature, 183 (1959) 1385.
6 A. Whitaker and J.W. Jeffery, Acta Crystallogr., B26 (1970) 1429.
7 K. Kato, M. Shiba, M. Nakamura and T. Ariyoshi, Rept. Inst. Medical Dental Engrg., 10 (1976) 45.
8 S. Takeda, S. Kawahara, M. Nakamura, K. Sogawa, S. Machara, H. Mori, M. Yokoyama, H. Takahashi and A. Yata, Shika Igaku, 42 (1979) 429.
9 R. Neiman and A.C. Sarma, J. Dental Res., 59 (1980) 1478.
10 B. El-Jazairi, Concrete, (1982) 12.
11 T. Sugama and L.E. Kukacka, Cem. Concr. Res., 13 (1983) 407.
12 T. Sugama and L.E. Kukacka, Cem. Concr. Res., 13 (1983) 499.
13 B.E.I. Abdelrazig, J.H. Sharp, P.A. Siddy and B. El-Jazairi, Proc. Br. Ceram. Soc., 35 (1984) 141.
14 B.E.I. Abdelrazig and J.H. Sharp, Cem. Concr. Res., 15 (1985) 921.
15 A.I. Vogel, A Textbook of Quantitative Inorganic Analysis, Longman, London, 1961, p. 575.
16 W.M. Dehn and E.O. Heuse, J. Am. Chem. Soc., 29 (1907) 1137.
17 S.J. Keihl and H.B. Hardt, J. Am. Chem. Soc., 55 (1933) 605.
18 H. Bassett and W.L. Bedwell, J. Chem. Soc., (1933) 854.
19 V. Auger and N. Ivanoff, C. R. Acad. Sci. Ser. C, 204 (1937) 434.
20 J. Paulik and F. Paulik, Proc. 4th Int. Conf. Thermal Analysis, Budapest, 1974, I. Buzas (Ed.), Akademiai Kiado, Budapest, 3 (1974) 789.
21 B.E.I. Abdelrazig, Ph.D. Thesis, University of Sheffield (1985).
22 P.A. Barnes, B.E.I. Abdelrazig and J.H. Sharp, unpublished results.